Efficiency Optimisation of an Experimental PEM Fuel Cell System via Super Twisting Control

Cristian Kunusch† Paul F. Puleston‡ Miguel A. Mayosky‡ Alejandro Dávila*

***Abstract*— A robust control solution is proposed to solve the air supply control problem in autonomous polymer electrolyte membrane fuel cells (PEMFC) based systems. Different second order sliding mode (SOSM) controllers are designed using a model of a laboratory test fuel cell generation system. Very good simulation results are obtained using such algorithms, showing the suitability of the SOSM approach to PEMFC stack breathing control. Subsequently, for experimental validation, a controller based on one of the previously assessed SOSM algorithms, namely a Super Twisting, is successfully implemented in the laboratory test bench. Highly satisfactory results are obtained, regarding dynamic behaviour, regulation error and robustness to uncertainties and external disturbances.**

I. INTRODUCTION

Increasing society concerns regarding the fundamental problems of the use of hydrocarbons [1] are soaring research on renewable power sources. Hydrogen, which is an efficient and clean energy carrier, is a viable solution to mitigate the problems associated to greenhouse gas emissions and source dependence. In future energy schemes, renewable energy sources will be fundamental and hydrogen can play a key role for efficiency enhancement. Considering that renewable energy sources are often intermittent and difficult to predict, it is usually difficult to match the energy production and the energy demand. Thus, the introduction of hydrogen as an energy vector helps this matching and allows increasing the efficiency and stability of the generation systems. Going from a hydrocarbon based energy system to a new scheme where hydrogen plays a basic role, naturally introduces fuel cells (FC) in the energy conversion chain. These devices produce electrical power through the catalytic reaction of hydrogen oxidation, they are highly efficient and their only by-products are water and heat. However, high costs, low reliability and short lifetime of fuel cells are still limiting its massive utilization in real applications. In this context, not only the improvement of the system design, better materials and components, but also new advanced control systems, are necessary to achieve costs reduction, faster dynamic responses, longer lifetimes and the optimization of the energy conversion.

Improving the dynamic response and efficiency of a fuel cell based system is a challenging control objective, as the FC itself involves the interaction of many high-order nonlinear components. For instance, a system comprising an air supply subsystem of a polymer electrolyte membrane (PEM) fuel cell stack connected to an air compressor is described by a seventh order nonlinear model [2], where many internal variables are inaccessible for its use in control algorithms. Besides, there are measurable and non-measurable disturbances that can affect system operation, as well as model uncertainties.

Then, reliable control systems ensuring stability and performance, as well as robustness to model uncertainties and external perturbations are of capital importance for FC success. In particular, the oxygen stoichiometry control system [3][4], has to be able to optimise the system conversion efficiency, avoiding performance deterioration together with eventual irreversible damages in the polymeric membranes. Therefore, an air flow control design and its implementation in a laboratory fuel cell system are presented in this work. The control problem is solved through second order sliding mode (SOSM) control. The potential of this design technique applied to fuel cells has been preliminary explored in [2], using an open literature model of a PEMFC system for automotive applications. Among some of the advantages of SOSM, it can be highlighted the capability of system robust stabilization, finite time convergence to the sliding surface and chattering reduction even in the presence of model uncertainties and disturbances [5][6][7].

Results provided in this paper can be easily extended to other PEMFC systems. In the current work simulation results show the suitability of SOSM to tackle this control problem while, its successful implementation in an actual fuel cell based generation system, experimentally demonstrates the viability of this control solution.

II. EXPERIMENTAL FUEL CELL SYSTEM

Details of the laboratory test station used for controller design and verification are shown if fig. 1. A schematic diagram of the system is portrayed in fig. 2, where sensors and actuators are also displayed. The main susbystems are

- Air Compressor: 12V DC oil-free diaphragm vacuum pump. Input voltage to this device is used as the main control action.
- Hydrogen and Oxygen humidifiers and line heaters: These are used to maintain proper humidity and temperature conditions inside the cell stack, an important issue for PEM membranes. Cellkraft® membrane exchange humidifiers are used in the current setup. Decentralized

† Institute of Robotics and Industrial informatics (IRI), research center of the Technical University of Catalonia (UPC) and the Spanish Council for Scientific Research (CSIC), Barcelona Technology Park, Spain. ckunusch@iri.upc.edu

‡ Laboratory of Industrial Electronics Control and Instrumentation (LEICI), Faculty of Engineering, National University of La Plata, La Plata, Argentine.

* Department of Control, Division of Electrical Engineering, Engineering Faculty, National Autonomous University of Mexico, DF, Mexico.

PID controllers in a power station ensure adequate operation values.

- Fuel cell stack: an ElectroChem® 7-cell stack with Nafion 115® membrane electrodes assemblies (MEAs) is used, with a catalyst loading of 1 mg/cm^2 of platinum, 50 cm^2 of active area, 50W of nominal power and 100W peak power.

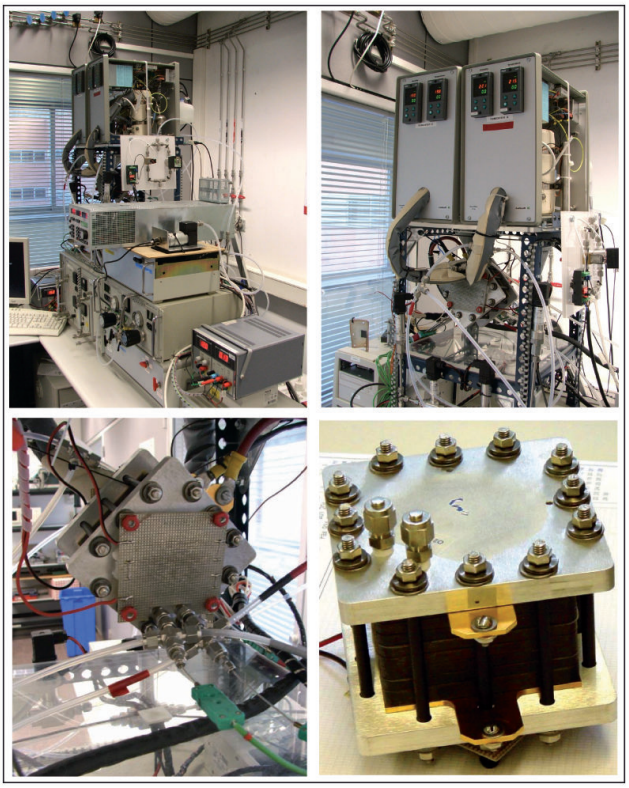

Fig. 1. Experimental PEM fuel cells laboratory at IRI (UPC-CSIC)

Different sensors are incorporated to measure specific variables, suited for modeling and control. Regarding fig. 2, these are: motor shaft angular velocity (ω_{cp}), compressor air mass flow (W_{cp}), hydrogen mass flow (W_{H2}), cathode and anode humidifiers pressures ($P_{hum,ca}$ and $P_{hum,an}$), stack pressure drops (P_{ca} and P_{an}), motor stator current (I_{cp}) and voltage (V_{cp}), stack voltage (V_{st}) and load current (I_{load}). Besides, a number of sensors were included to register significant temperatures (T_{st}, $T_{hum,ca}$, $T_{lh,ca}$, $T_{hum,an}$ and $T_{lh,an}$). It must be noted that in a typical fuel cell application many of these measurements are not necessary. For instance, the controller proposed in section 5 only requires measurement of the stack current and the compressor air flow.

System modelling was performed by the authors combining theoretical techniques and empirical analysis. Dynamic models of the compressor, cathode and anode humidifier, line heaters, fuel cell stack channels and membrane water transport were developed and experimentally validated. The resulting model, suitable for SOSM control design, has the

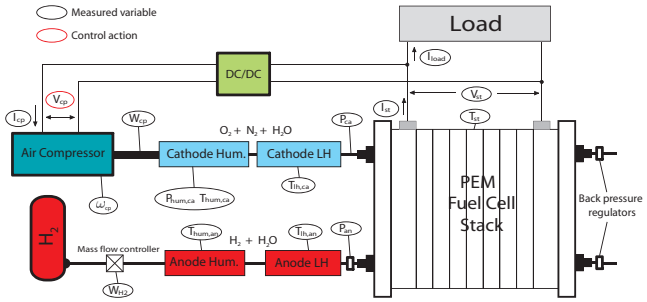

Fig. 2. PEM Fuel cell system schematics

following general form:

$$\dot{x} = F(x(t)) + G \cdot u(t)$$

where $X_1 = [x_1\ x_2\ x_3\ x_4\ x_5\ x_6\ x_7] \in \mathscr{R}^7$ and $u \in \mathscr{R}$.

- $x_1 = W_{cp}$: compressor air mass flow [kg/s].
- $x_2 = m_{hum,ca}$: mass of air in the cathode humidifier [kg].
- $x_3 = m_{o_2,ca}$: mass of oxygen in the stack cathode [kg].
- $x_4 = m_{N_2,ca}$: mass of nitrogen in the stack cathode [kg].
- $x_5 = m_{v_2,ca}$: mass of vapour in the stack cathode [kg].
- $x_6 = m_{H_2,an}$: mass of hydrogen in the stack anode [kg].
- $x_7 = m_{v_2,an}$: mass of vapour in the stack anode [kg].

The complete set of equations and physical parameters is not included here for space reasons and can be found in [8] and [9]

III. Control Objective and Sliding Surface

As already stated, the main objective of the control strategy proposed is the optimization of the energy conversion of the fuel cell, maximizing the net power generated by the system under different load conditions. Considering that the compressor is also driven by the fuel cell (in fact, it can be regarded as a parasitic load), the output net power (P_{net}) can be defined as the electrical power delivered by the stack ($P_{st} = V_{st} I_{st}$) minus the electrical power consumed by the compression subsystem ($P_{cp} = V_{cp} I_{cp}$). Optimization of the system efficiency can be achieved by regulating the air mass flow entering to the stack cathode at different load conditions.

Accomplishing such optimal comburent flow is equivalent to maintaining the cathode line oxygen stoichiometry in an optimal value. This becomes evident from fig. 3. The optimum value of λ_{o_2} can be determined from a thorough analysis of the open loop system, considering changes in the current demanded to the stack and a wide set of stoichiometry values.

The oxygen stoichiometry or oxygen excess ratio is defined as:

$$\lambda_{o_2} = \frac{W_{o_2,in}}{W_{o_2,react}} \tag{1}$$

where $W_{o_2,in}$ is the oxygen partial flow in the cathode, which depends on the air flow released by the compressor W_{cp} and the vapour injected by the humidifier. $W_{o_2,react}$ is the oxygen flow consumed in the reaction. It can be directly related to

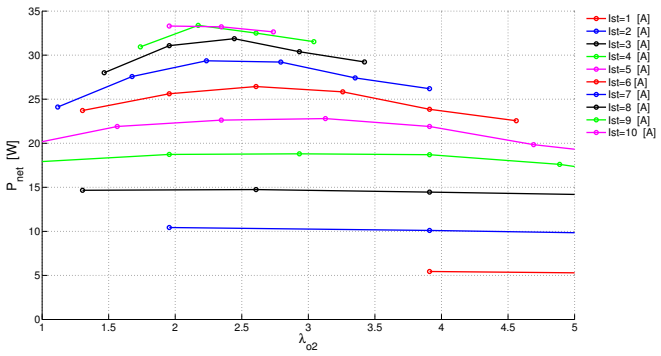

Fig. 3. System performance in different load conditions (P_{net} vs. λ_{o2})

the total stack current (I_{st}):

$$W_{o_2,react} = G_{o_2} \frac{nI_{st}}{4F} \tag{2}$$

G_{o2} is the molar mass of oxygen, n the total number of cells of the stack and F the Faraday constant.

Once $\lambda_{o_2,opt}$ is determined, the objective of keeping the oxygen excess ratio within optimal values can be achieved controlling the oxygen mass flow ($W_{o_2,in}$). Then, the following mass flow reference can be obtained from (1) and (2):

$$W_{o_2,in,ref} = \lambda_{o_2,opt} M_{o_2} \frac{nI_{st}}{4F} \tag{3}$$

where tracking $W_{o_2,in,ref}$ effectively implies $\lambda_{o_2} = \lambda_{o_2,opt}$.

In the framework of the sliding mode theory, this control objective can be expressed as follows:

$$S(x,t) = W_{cp} - W_{cp,ref} \tag{4}$$

where S is the sliding variable that must be steered to zero and $W_{cp,ref}$ is the compressor air mass flow reference. This latter expression can be readily obtained from the air mass flow reference. Given that the molar fraction of oxygen in the air (χ_{o2}) is known, the desired mass flow of dry air can be directly computed from:

$$W_{dry\ air,ref} = \frac{1}{\chi_{o2}} W_{o_2,in_{ref}} = \frac{1}{\chi_{o2}} \lambda_{o_2,opt} M_{o_2} \frac{nI_{st}}{4F} \tag{5}$$

Then, taking into account the relative humidity of the air (Ω_{atm}), the final expression of the air mass reference results:

$$W_{cp,ref} = (1 + \Omega_{atm}) \frac{1}{\chi_{o2}} \lambda_{o2,opt} M_{o2} \frac{nI_{st}}{4F} \tag{6}$$

Note that for stable ambient conditions, the reference only depends on a single measurable variable, i.e. the stack current I_{st}.

IV. Design of PEMFC-SOSM controllers

It has been established in Section I that SOSM techniques present attractive characteristics that well suit the PEMFC breathing control requirements. Together with the general features of robustness, finite time convergence and chattering reduction, in particular, generation of continuous control action signals avoid output power quality deterioration and the inconvenience of discontinuous voltage directly applied to the compressor input.

A battery of SOSM algorithms can be found in the literature, each one of them with its distinctive features. In this work, three of the most well-known among them, namely Twisting, Sub-Optimal and Super Twisting, have been chosen to evaluate the viability of the SOSM approach to this fuel cell system. To this aim, the controllers have been designed using (1) (the detailed model description is given in [8]) and have been assessed by thorough simulation tests. To obtain the controllers gains, an initial design procedure, common to the three algorithms, must be followed. To begin with, the first and second time derivatives of the sliding variable (4) have to be computed. They can be expressed as:

$$\dot{S} = \frac{\partial}{\partial t} S(t,x) + \frac{\partial}{\partial x} S(t,x).(F(x) + G) \tag{7}$$

$$\ddot{S} = \frac{\partial}{\partial t} \dot{S}(t,x,u) + \frac{\partial}{\partial x} \dot{S}(t,x,u).(F(x) + G) + \\ + \frac{\partial}{\partial u} \dot{S}(t,x,u).\dot{u}(t) = \varphi(t,x,u) + \gamma(t,x,u)\dot{u}(t) \tag{8}$$

where $\varphi(t,x,u)$ and $\gamma(t,x,u)$ for the PEMFC system are smooth functions, that have to be bounded as follows:

$$0 < \Gamma_m \leq \gamma(t,x,u) \leq \Gamma_M \tag{9}$$

$$|\varphi(t,x,u)| \leq \Phi \tag{10}$$

For the PEMFC under study, the bounding values were computed by a numerical study of the nonlinear system and refined through a physical study. Additionally, some uncertainties were included in representative parameters such as the motor inertia, torque friction, humidifier volume and cathode air constant. The following values were obtained:

$$\Phi = 2.310^{-5}; \quad \Gamma_m = 0,002; \quad \Gamma_M = 0,0083 \tag{11}$$

Once the bounds have been determined, the stabilization problem of system (1) with input-output dynamics (8) can be solved through the solutions of the following equivalent differential inclusion by applying SOSM:

$$\ddot{s} \in [-\Phi, \Phi] + [\Gamma_m, \Gamma_M]\dot{u} \tag{12}$$

Then, the gains of the SOSM algorithms are calculated from Φ, Γ_m and Γ_M guaranteeing that, once the system is steered to the region where they hold, the trajectories do not escape and converge to $S = \dot{S} = 0$ in $t < \infty$.

The algorithms used in this paper depend on few parameters, which are computed during the off-line tuning procedure. Thus, the on-line operation of the control algorithms is very simple and with low computational cost. In particular, the first two algorithms are intended for a sliding variable of relative degree 2. Given that in the PEMFC under consideration the relative degree is 1, for these first two cases the system has been expanded with an integrator, considering $\dot{u}(t)$ as the control action for the design. The algorithms and the chosen gains for the PEMFC controllers are succinctly described below.

A. Twisting Algorithm

This algorithm is characterised by the manner in which its trajectories converge to the origin in the sliding plane $S-\dot{S}$. The knowledge of the signs of S and $\dot{S}$ is needed. The control law is given by [10]:

$$v(t) = \dot{u}(t) = -r_1 sign(S) - r_2 sign(\dot{S}) \tag{13}$$

Sufficient conditions for finite-time convergence can be stated as:

$$\begin{gathered} r_1 > r_2 > 0 \\ (r_1 + r_2)\Gamma_m - \Phi > (r_1 - r_2)\Gamma_M + \Phi \\ (r_1 - r_2) > \frac{\Phi}{\Gamma_m} \end{gathered} \tag{14}$$

Therefore, the chosen gains result:

$$r_1 = 1.75 \;\; ; \;\; r_2 = 1.25 \tag{15}$$

B. Sub-optimal Algorithm

Trajectories in the $S-\dot{S}$ plane are confined within parabolic arcs which include the origin, so the convergence behaviour may execute twisting around the origin, "bouncing" on the S axis or a combination of both. Its control law is [11]:

$$\begin{gathered} v(t) = \dot{u}(t) = \alpha(t) U sign(S - \beta\sigma_M) \\ \alpha(t) = \begin{cases} 1 & si \quad (S-\beta\sigma_M)\sigma_M \geq 0 \\ \alpha^* & si \quad (S-\beta\sigma_M)\sigma_M < 0 \end{cases} \end{gathered} \tag{16}$$

where $U > 0$ is the control authority, $\alpha^* > 1$ is the modulation parameter, $0 \leq \beta < 1$ is the anticipation parameter and σ_M is a piece-wise constant function representing the last extremal value of the sliding variable $S(t)$.

Convergence in finite time is guaranteed if:

$$\begin{gathered} U > \frac{\Phi}{\Gamma_m} \\ \alpha^* \in [1; +\infty) \cap \left[\frac{\Phi + (1-\beta)\Gamma_M U}{\beta \Gamma_m U}; +\infty \right) \end{gathered} \tag{17}$$

This algorithm requires the ability to detect the times when $\dot{S}$ become zero and the corresponding values of S in those instants, i.e. σ_M. The final choice of the controller parameters for the PEMFC system is:

$$\alpha^* = 18 \;\; ; \;\; U = 0.5 \;\; ; \;\; \beta = 0.2 \tag{18}$$

C. Super Twisting Algorithm

This algorithm is intended to systems with relative degree 1. One interesting feature is that, during on-line operation, it does not require information of $\dot{\sigma}$. The trajectories converge to the origin of the sliding plane turning around in a typical way. The control law comprises two terms. One is the integral of a discontinuous control action and, the other, is a continuous function of S, contributing only during the reaching phase [12]:

$$\begin{gathered} u(t) = u_1(t) + u_2(t) \\ \dot{u}_1(t) = -\gamma sign(S) \\ u_2(t) = \begin{cases} -\lambda |S_0|^{1/2} sign(S) \;\; if & |S| > |S_0| \\ -\lambda |S|^{1/2} sign(S) \;\; if & |S| \leq |S_0| \end{cases} \end{gathered} \tag{19}$$

where γ and λ are design parameters that where derived from the corresponding sufficient conditions for finite time convergence of the algorithm [12]:

$$\begin{gathered} \gamma > \frac{\Phi}{\Gamma_m} \\ \lambda > \sqrt{\frac{2}{\Gamma_m^2} \frac{(\Gamma_m \gamma + \Phi)^2}{(\Gamma_m \gamma - \Phi)}} \end{gathered} \tag{20}$$

Among the gains that fulfil them, best performance have been achieved with:

$$\lambda = 20 \;\; ; \;\; \gamma = 0,08 \tag{21}$$

It was previously stated that it is necessary to define an extra control action that steers the sliding variable within a region such that the bounds on the sliding dynamics given in (9-10) are satisfied [5]. With this purpose, a feedforward action u_{ff} has been included. It provides the control effort required to reach the surface neighborhood ($S < |S_0|$) where conditions (9-10) hold. Therefore, the implemented control action (u_i) comprises two terms:

$$u_i(t) = u_{ff} + u \tag{22}$$

where u corresponds to the SOSM control action particularised above. The expression of u_{ff} is computed via a polynomial obtained from an off-line test along the entire operation range of the PEMFC system and given by:

$$\begin{aligned} u_{ff} \;\; &= \;\; 0.1014 \; W_{cp,ref}^6 - 1.1412 \; W_{cp,ref}^5 + \\ &+ \;\; 4.8303 \; W_{cp,ref}^4 - 9.3370 \; W_{cp,ref}^3 + \\ &+ \;\; 8.1430 \; W_{cp,ref}^2 - 0.6129 \; W_{cp,ref} - 0.1934 \end{aligned} \tag{23}$$

In the following figures it is presented the simulations results of the controlled system using the algorithms designed above. In figure (4) it is shown that the Twisting, Sub-Optimal and Super Twisting controllers present a satisfactory dynamic response when controlling the air mass flow. In figure (4), the typical behaviour that impose the algorithms to the nonlinear system is shown through as S-$\dot{S}$ diagram. It is important to stress that, in simulations tests, the three controllers present a similar dynamic behaviours when at similar parameters tuning, so the suitability of the SOSM approach for the breathing control of this PEMFC system it is verified.

V. Experimental results

Among several simulation and experimental tests performed in the fuel cell system, a first approach to solve the real problem was implemented through a Super Twisting controller. Considering that the plant has a relative degree one and a noisy control output, the selected algorithm is particularly suitable for the current laboratory implementation.

One of the objectives of this section is to present the performance of the proposed SOSM controller, implemented in the fuel cell test station and considering external disturbances and different working conditions.

To assess the controller performance in real operation, in figure (6) it can be appreciated the performance of the SOSM+FF controller at different load conditions. Comparing

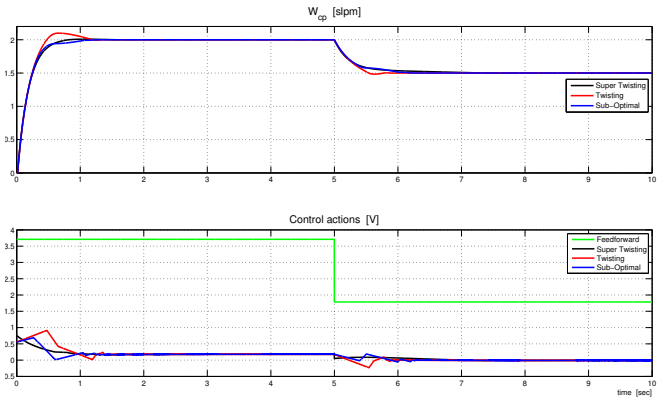

Fig. 4. Air flow and control input (simulation results)

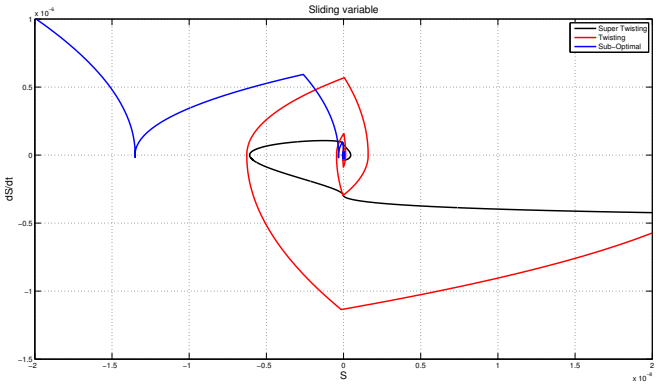

Fig. 5. S vs. $\dot{S}$ (simulation results)

figures (6) and (4), it can be stated that the simulation and experimental results preserve the same dynamic behaviour, showing the reliability and accuracy of the design methodology.

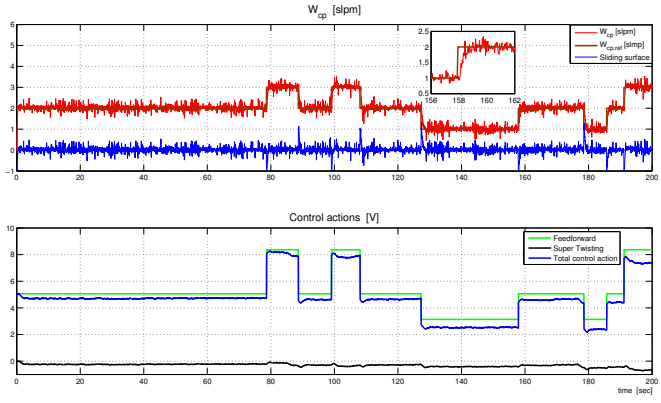

Fig. 6. W_{cp} regulation with SOSM+FF controller (experimental results)

Another representative set of tests was performed in the PEM fuel cell test station, considering a external perturbation in the cathode line pressure. In these experiments, the control performance was assessed at a fixed control reference, see figure (7), while a pressure disturbance in the air pressure was incorporated by means of an electronic valve.

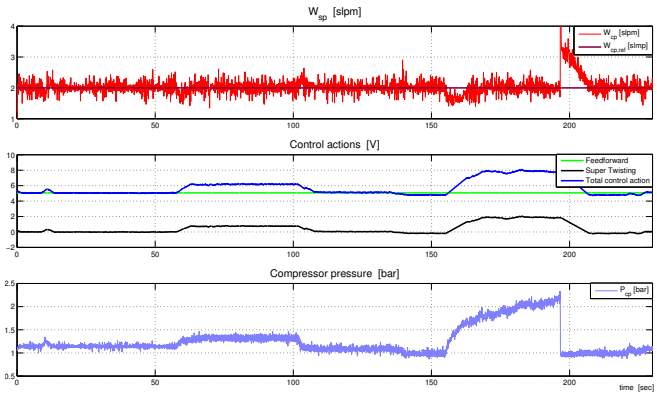

Fig. 7. Perturbation test (experimental results)

It can be noticed that the control objective is satisfactory accomplished during the imposed perturbation. Moreover, when the system is strongly perturbed ($t \simeq 195$ s), the controller drives again the system trajectories to the sliding surface. This effect is achieved because the stability of the closed loop system is guaranteed given that the differential inclusion (12) is satisfied.

It is important to mention that the proposed SOSM+FF controller showed very good performance for a wide range of operation conditions, proving robustness with respect to external disturbances and model uncertainties. Apart from the presented examples, extensive simulation and experimental analysis have been conducted and, in every case, highly satisfactory results have been obtained using the proposed SOSM controllers.

VI. Conclusions

Different high order sliding mode controllers that globally solve the oxygen stoichiometry problem of a laboratory PEMFC generation system were designed in this paper. Their suitability was successfully verified through computer simulation, taking into account external disturbances and uncertainties in the system parameters. Subsequently, highly satisfactory experimental results using the aforementioned approach, particularly a Super Twisting topology with feedforward action, confirm the feasibility and simplicity of the solution. Main advantages of the proposed SOSM control for PEMFC systems can be summarized as follows:

- solution of the robust stabilization problem avoiding chattering effects;
- enhanced dynamic characteristics;
- robustness to parameter uncertainties and external disturbances;
- guaranteed extended range of operation, in spite of the highly nonlinear nature of plant;
- the control law only depends on two measurable variables, namely the stack current and the compressor air flow, therefore no observer or state estimation is required;

- simple controller structure, resulting in low real time computational costs.

The resulting controllers were relatively simple to design from measurements that can be easily taken from the real system. This is an important issue for industrial applications, where instrumentation must be kept to a minimum.

VII. ACKNOWLEDGMENTS

We would like to thank the members of the Institut de Robòtica i Informàtica Industrial (CSIC-UPC), where all the experimental tests were conducted. The work was supported by CICYT project DPI2007-62966 (MICINN-España), AECID project A/026279/09, Universidad Nacional de La Plata (Argentina), CONICET, CICPBA and ANPCyT.

REFERENCES

[1] F. Barbir, *PEM fuel cells: theory and practice*. Elsevier, 2005.

[2] C. Kunusch, P. Puleston, M. Mayosky, and J. Riera, "Sliding mode strategy for pem fuel cells stacks breathing control using a super-twisting algorithm," *IEEE Transactions on Control System Technology*, vol. 17, pp. 167–174, 2009.

[3] J. Pukrushpan, A. Stefanopoulou, and H. Peng, *Control of Fuel Cell Power Systems*. Springer, 2004.

[4] J. Larminie and A. Dicks, *Fuel Cell Systems Explained*, 2nd ed. John Wiley & Sons Inc, 2003.

[5] L. Fridman and A. Levant, *Sliding Mode Control in Engineering*. Marcel Dekker, Inc., 2002, ch. 3 "Higher Order Sliding Modes", pp. 53–101.

[6] G. Bartolini, A. Ferrara, and E. Usai, "Chattering avoidance by second order sliding mode control," *IEEE Transactions on Automatic Control*, vol. 43, no. 2, pp. 241–246, 1998.

[7] I. Boiko and L. Fridman, "Analysis of chattering in continuous sliding-mode controllers," *IEEE Transactions on Automatic Control*, vol. 50, no. 9, pp. 1442–1446, September 2005.

[8] C. Kunusch, P. Puleston, M. Mayosky, and A. Husar, "Modelado dinmico y validación experimental de una pila de combustible PEM," in *XIII Congreso Latinoamericano de Control Automtico*, Mérida, Venezuela, November 2008.

[9] C. Kunusch, "Modelling and nonlinear control of PEM fuel cell systems (in spanish)," Ph.D. dissertation, Electrical Department, National University of La Plata, September 2009.

[10] G. Bartolini, A. Ferrara, and E. Levant, A. andUsai, *Variable structure systems, sliding mode and nonlinear control*. Berlin: Springer Verlag, 2007, no. 274, ch. On second order sliding mode controllers, pp. 329–350.

[11] G. Bartolini and P. Pydynowsky, "An improved chattering free VSC scheme for uncertain dynamical systems," *IEEE Transactions on Automatic Control*, vol. 41, no. 4, pp. 1220–1226, 1996.

[12] A. Levant, "Sliding order and sliding accuracy in sliding mode control," *International Journal of Control*, vol. 58, no. 6, pp. 1247–1263, 1993.